J. Fluid Mech. (1992), *vol.* 238, *pp.* 467–486
Printed in Great Britain

On the multifractal properties of the energy dissipation derived from turbulence data

By E. AURELL[1,2], U. FRISCH[2], J. LUTSKO[3] AND M. VERGASSOLA[2,4]

[1] Department of Mathematics, KTH, 10044 Stockholm, Sweden

[2] CNRS, Observatoire de Nice, B.P. 229, 06304 Nice Cedex 4, France

[3] Physique Non-Linéaire et Mécanique Statistique, Univ. Libre de Bruxelles, C.P. 231, 1050 Brussels, Belgium

[4] Dipartimento di Fisica, Universitá di Roma 'La Sapienza', P.le A. Moro 2, I-00185 Rome, Italy

(Received 12 October 1991)

Various difficulties can be expected in trying to extract from experimental data the distribution of singularities, the $f(\alpha)$ function, of the energy dissipation. One reason is that the multifractal model of turbulence implies a dependence of the viscous cutoff on the singularity exponent. It is an open question if current hot-wire probes can resolve the scales implied by exponents α significantly less than 1.

Two exactly soluble models are used to show how spurious scaling can occur, due to finite Reynolds number effects. In the Gaussian model the true velocity signal is replaced by independent Gaussian random variables. The dissipation, defined as the square of the difference of successive variables, has trivial scaling in so far as all the moments of spatial averages of the dissipation behave asymptotically as a uniform dissipation. Still, contamination by subdominant terms requires that scaling exponents for high-order moments be identified over an increasingly large range of scales. If the available range is limited by the Reynolds number, scaling exponents for high orders will be systematically underestimated and spurious intermittency will be inferred. Burgers' model is used to highlight further problems. At finite Reynolds numbers, regions with no small-scale activity (away from shocks) have a residual dissipation which contributes a spurious point ($\alpha = 1, f(\alpha) = 1$). In addition, when the $f(\alpha)$ function is obtained by Legendre transform techniques, convex hull effects generate an entire spurious segment.

Finally, Burgers' model also indicates that the relation between exponents of structure functions and exponents of local dissipation moments, which goes back to Kolmogorov's (1962) work, leads to an inconsistency for structure functions of low positive order.

1. Introduction

In the early 1960s, Oboukhov (1962) and Kolmogorov (1962) proposed a modification of the celebrated Kolmogorov (1941*a*) theory. They assumed that spatial fluctuations of the energy dissipation are 'intermittent', that is, increase when considering finer and finer scales in the inertial range. They showed how such fluctuations can lead to scaling laws for structure functions which deviate from the K41 predictions. For a modern perspective on the history of intermittency, the reader is referred to Frisch (1991) and other papers in the special issue of *Proc. Roy.*

Soc. A devoted to A. N. Kolmogorov (vol. 434, 1991, pp. 9–217). Here, we shall comment only on aspects of this subject directly relevant to our present study. It has been observed by Parisi & Frisch (1985) that an alternative description of intermittency is through the spectrum of singularities of the velocity field. In the Parisi & Frisch *multifractal* model it is assumed that the singularities can be characterized by a continuous range of scaling exponents h. For any h in this range, there is a set $\mathscr{S}_h$ in $\boldsymbol{R}^3$ of Hausdorff dimension $D(h)$ such that, when $\boldsymbol{r}\in\mathscr{S}_h$, the velocity increment

$$\delta\boldsymbol{v}(\boldsymbol{r},l\boldsymbol{e}) = \boldsymbol{v}(\boldsymbol{r}+l\boldsymbol{e})-\boldsymbol{v}(\boldsymbol{r}) \tag{1}$$

behaves for small l (in the inertial range) as

$$\frac{|\delta\boldsymbol{v}(\boldsymbol{r},l\boldsymbol{e})|}{v_0}\sim\left(\frac{l}{l_0}\right)^h \quad \text{for} \quad \boldsymbol{r}\in\mathscr{S}_h\subset\boldsymbol{R}^3; \quad \dim\mathscr{S}_h = D(h). \tag{2}$$

Here, v_0 is the r.m.s. fluctuating velocity, l_0 the integral scale, $\boldsymbol{e}$ is an arbitrary unit vector and $D(h)$ is assumed to be universal. This multifractal assumption leads to a set of scaling exponents ζ_p for the structure function of order p. The function ζ_p is essentially the Legendre transform of $D(h)$. A general class of cascade models of intermittency, introduced by Mandelbrot (1974) and generalizing models due to the Russian school (see Monin & Yaglom 1975), was reinterpreted by Parisi & Frisch (1985) in terms of local scaling exponents. Recently, this led to a prediction of a new form of universality for the dissipation range, permitting in principle the measurement of $D(h)$ from the energy spectrum (Frisch & Vergassola 1991). This prediction has already received some experimental validation (Gagne & Castaing 1991). Similar universality has also been observed in a convection experiment (Wu *et al.* 1990).

The concept of multifractality has proved particularly fruitful in the characterization of attractors in dynamical systems (Benzi *et al.* 1984; Halsey *et al.* 1986). Very accurate measurements of the distribution of singularities (called $f(\alpha)$) have permitted detailed confirmation of theoretical predictions (Bensimon, Jensen & Kadanoff 1986; Glazier *et al.* 1986). Actually, the concept of a multifractal originated from an attempt to interpret experimental data on fully developed turbulence (Anselmet *et al.* 1984). Still, the experimental difficulties in measuring the distribution of (quasi)singularities in physical space-time for fully developed turbulence are far greater than the measurement of singularities of attractors in phase space for low-dimensional dynamical systems.

It is our purpose, here, to analyse from a theoretical viewpoint some of the difficulties one can encounter in extracting the multifractal properties of the energy dissipation from experimental data, as was attempted in the pioneering work of Meneveau & Sreenivasan (1987, 1991). Our paper is organized as follows. Section 2 is devoted to the relations between two multifractal descriptions of turbulence, one operating at the level of structure functions and the other at the level of the energy dissipation. In §3 we discuss general principles involved in obtaining the so-called $f(\alpha)$ function from one-dimensional cuts. In §§4 and 5 we list and then discuss the main approximations involved in the practical procedures used. Specific difficulties are highlighted by studying two exactly soluble models in §§6 and 7. Concluding remarks are made in §8.

2. The two approaches to multifractals in turbulence

Some of the material in this Section is well-known and is covered in more detail, for example, in Meneveau & Sreenivasan (1987).

The Parisi & Frisch formalism works entirely with inertial-range quantities. From the basic assumptions of homogeneity, isotropy and of local scaling with exponent h on sets of Hausdorff dimensions $D(h)$, it follows that the longitudinal *structure function* of order p,

$$S_p(l) = \langle (\boldsymbol{e}\cdot\delta\boldsymbol{v}(\boldsymbol{r}, l\boldsymbol{e}))^p \rangle, \tag{3}$$

behaves in the inertial range as a power law:

$$S_p(l) \propto l^{\zeta_p} \quad \text{with} \quad \zeta_p = \min_h (ph+3-D(h)). \tag{4}$$

Of course (4) is valid only over inertial-range scales. It must be stressed that the extent of the inertial range depends on the order of the structure function under consideration. Indeed, under the assumption of convexity, $D''(h) < 0$, there is a single scaling exponent $h_*(p)$ which minimizes $ph+3-D(h)$. Unless $D(h)$ is a trivial function (as in Kolmogorov 1941*a*), $h_*(p)$ will vary with p. A simple turnover-time argument (Paladin & Vulpiani 1987) shows that the viscous cutoff η depends on the scaling exponent h through

$$\frac{\eta(h)}{l_0} \sim R^{-1/(1+h)}, \tag{5}$$

where $R = l_0 v_0/\nu$ is the Reynolds number (ν being the kinematic viscosity). It follows that, at high Reynolds numbers, scales much smaller than the Kolmogorov scale, obtained by setting $h = \frac{1}{3}$ in (5), are relevant in studying multifractal properties. The relation (5) has also been noted by Meneveau & Nelkin (1989) and has been used by Frisch & Vergassola (1991). Experimental attempts to check (5) are now being made (see e.g. Van de Water, Van der Vorst & Van de Wetering 1991).

We turn now to the second form of multifractality, based on the energy dissipation. Here, the key quantity is the spatial average of the energy dissipation over a ball of radius l centred at the point $\boldsymbol{r}$, first considered by Oboukhov (1962) and Kolmogorov (1962):

$$\epsilon_l(\boldsymbol{r}) = \frac{1}{\frac{4}{3}\pi l^3} \int_{|\boldsymbol{r}'-\boldsymbol{r}|<l} \mathrm{d}^3\boldsymbol{r}' \tfrac{1}{2}\nu \sum_{ij} (\partial_j v_i(\boldsymbol{r}') + \partial_i v_j(\boldsymbol{r}'))^2. \tag{6}$$

It is now assumed that, when the viscosity ν is small, $\epsilon_l(\boldsymbol{r})$ has the *multifractal property*. This means, roughly, that

$$\frac{\epsilon_l(\boldsymbol{r})}{v_0^3/l_0} \sim \left(\frac{l}{l_0}\right)^{\alpha-1} \quad \text{as} \quad l\to 0 \quad \text{for} \quad \boldsymbol{r}\in\mathscr{D}_\alpha \subset \boldsymbol{R}^3; \quad \dim \mathscr{D}_\alpha = F(\alpha). \tag{7}$$

Note that $\epsilon_l(\boldsymbol{r})$ and l have been respectively divided by v_0^3/l_0 (the order of magnitude of the mean dissipation) and l_0 (the integral scale) to obtain dimensionless quantities. By a standard steepest-descent argument, it follows now that for small l

$$\lim_{\nu\to 0} \langle \epsilon_l^q \rangle \sim \left(\frac{v_0^3}{l_0}\right)^q \left(\frac{l}{l_0}\right)^{\tau_q}, \quad \tau_q = \min_\alpha [q(\alpha-1)+3-F(\alpha)]. \tag{8}$$

Note that the averaging in (8) is typically a time average, implying the limit $t\to\infty$, which must be taken before the limit $\nu\to 0$; the limit $l\to 0$ being taken last. Any other order could lead to contradictions.

We now observe that Kolmogorov (1962) proposed to relate the fluctuations of velocity increments and those of the space-averaged dissipation. His 'first and second hypotheses' imply the following result for the asymptotic behaviour when $l \to 0$ (after the limit $\nu \to 0$ has been taken):

$$\boldsymbol{e} \cdot \delta \boldsymbol{v}(\boldsymbol{r}, l\boldsymbol{e}) =^{\mathrm{s}} (\epsilon_l(\boldsymbol{r})\, l)^{\frac{1}{3}}. \tag{9}$$

Here, the symbol $=^{\mathrm{s}}$ means that the two quantities have the same scaling properties, so that the scaling exponents are the same for corresponding moments of arbitrary order. Equation (9) is essentially the Kolmogorov (1941*a*) assumption, reformulated locally in terms of fluctuating quantities. This assumption is clearly consistent from the viewpoint of dimensional analysis. Furthermore, the third-order moments of the left- and right-hand sides of (9) have exactly the same scaling (proportional to l^1) as follows from Kolmogorov's '$-\frac{4}{5}$' relation for the third-order structure function (Kolmogorov 1941*b*; see also Frisch 1991). Still, (9) has never been established convincingly. Bacry *et al.* (1990) have questioned its validity when it is used to evaluate moments of negative orders. On Burgers' model it may be shown that inconsistencies arise for moments of positive fractional orders less than 1 (see §7).

Equation (9) has been mostly taken for granted and immediately implies that one can bridge the two multifractal formalisms described above. Indeed, it follows from (2), (4), (7), (8) and (9) that

$$h = \tfrac{1}{3}\alpha, \quad D(h) = F(\alpha), \quad \zeta_p = \tfrac{1}{3}p + \tau_{p/3}. \tag{10}$$

Similarly, the viscous cutoff, given by (5), can be re-expressed in the energy dissipation multifractal formalism as (the subscript 'diss' stands for 'dissipation')

$$\frac{\eta_{\mathrm{diss}}(\alpha)}{l_0} = R^{-3/(3+\alpha)}. \tag{11}$$

In bridging the two multifractal formalisms, we have chosen notation which preserves (i) the standard Kolmogorov definition of $\epsilon_l(\boldsymbol{r})$ and (ii) the equality of the two dimensions $F(\alpha)$ and $D(h)$ of (presumably) identical fractals in $\boldsymbol{R}^3$.

Very accurate and independent measurements of $(D(h), \zeta_p)$ and of $(F(\alpha), \tau_q)$ will be needed to find out more about the validity of Kolmogorov's relation (9).

3. The singularity spectrum from one-dimensional cuts

A genuine three-dimensional processing of turbulence data to measure the multifractal properties of the energy dissipation is at the moment feasible only for numerically simulated flows. These are however limited in Reynolds numbers to regimes where scaling just begins to manifest itself, thus making reliable measurements of multifractal properties difficult. Present experimental techniques have access to the two-dimensional structure of passive scalars (Prasad, Meneveau & Sreenivasan 1989; Miller & Dimotakis 1991) and only to the one-dimensional structure of the velocity field. Here, we are only interested in the latter. Mandelbrot (1974) has shown that for homogeneous fractals of dimension F, the fractal dimension f of one-dimensional cuts is $f = F - 2$. This relation remains valid (in so far as f controls probabilities) even when f becomes negative (Mandelbrot 1991). In processing the energy dissipation it is usually assumed that it behaves as a homogeneous multifractal, as far as its statistical properties (in the limit of zero viscosity) are concerned. Thus, one-dimensional space averages of the dissipation can

be used as 'representatives' of the three-dimensional averages. Specifically, one considers a one-dimensional line $\boldsymbol{L}$ with coordinate x and, instead of (6), one uses

$$\epsilon_l(x) = \frac{1}{2l}\int_{|x'-x|<l} \mathrm{d}x' \tfrac{1}{2}\nu \sum_{ij} (\partial_j v_i(x') + \partial_i v_j(x'))^2. \tag{12}$$

Similarly, instead of (7), it is assumed that, for small ν, $\epsilon_l(x)$ behaves as follows:

$$\frac{\epsilon_l(x)}{v_0^3/l_0} \sim \left(\frac{l}{l_0}\right)^{\alpha-1} \quad \text{as} \quad l\to 0 \quad \text{for} \quad x\in\mathscr{D}'_\alpha; \quad \dim \mathscr{D}'_\alpha = f(\alpha), \tag{13}$$

where $\mathscr{D}'_\alpha = \mathscr{D}_\alpha \cap \boldsymbol{L}$ and

$$f(\alpha) \equiv F(\alpha) - 2. \tag{14}$$

To recover the function $f(\alpha)$ from measurements of the fluctuating local dissipation $\epsilon_l(x)$, there are two main strategies.

The *moment method* has the following steps: (i) measure $\langle(\epsilon_l)^q\rangle$, in principle for arbitrary real q – the average can be taken over time; (ii) find the asymptotic behaviour for $l\to 0$ and identify its leading order with a power law $\propto l^{\tau_q}$; (iii) perform an inverse Legendre transform to obtain

$$f(\alpha) = \min_q [q(\alpha-1)+1-\tau_q]. \tag{15}$$

This relation is obtained by inversion of (8) and use of (14).

The *binning method* comprises the following steps: (i) measure the probability distribution function (p.d.f.) $P(\epsilon, l)$ of ϵ_l for given l; (ii) plot $\ln P(\epsilon, l)/\ln l$ *vs.* $\ln(l\epsilon)/\ln l$ for different l; (iii) in the limit $l\to 0$, all the plots collapse onto a single graph which corresponds to the map $\alpha \mapsto 1-f(\alpha)$.

The practical procedure is somewhat more elaborate because of the need to define binning intervals for the dissipation and the need to correct for the finiteness of the external scale (here, the integral scale l_0). For details, see Grassberger, Badii & Politi (1988); Politi, Badii & Grassberger (1988); Meneveau & Sreenivasan (1989).

4. Obtaining $f(\alpha)$ from experimental data

All existing attempts to measure $f(\alpha)$ for the velocity field are based on hot-wire techniques in the presence of a mean flow (wind tunnels, jets, etc.). In order to discuss the possible problems in the determination of $f(\alpha)$, we shall briefly review the main approximations involved in the experimental process. We shall concentrate on what we called in §3 the 'moment method'. The limitations for the 'binning method' are quite similar.

We shall not, here, be concerned with novel non-intrusive techniques which are still under development and have the potential of avoiding some of the difficulties we shall now stress.

In practice, the determination of $f(\alpha)$, as described in §2, has to be accompanied by some approximations which are now listed (without trying to be exhaustive).

(i) Assume a fixed, small, viscosity ν, i.e. drop the operation $\lim_{\nu\to 0}$ in (8).

(ii) Instead of the full squared deformation tensor appearing in (12), use just $(\partial u/\partial x)^2$, the square of the streamwise derivative of the streamwise velocity component.

(iii) Use the Taylor hypothesis to substitute time derivatives for space derivatives:

$$\frac{\partial u}{\partial x} \approx -\frac{1}{\bar{U}}\frac{\partial u}{\partial t}, \tag{16}$$

where $\bar{U}$ is the mean velocity.

(iv) Approximate time derivatives by time differences over the sampling time δt of the probe-recorded signal u_{P}:

$$\frac{\partial u}{\partial t} \approx \frac{1}{\delta t}[u_{\mathrm{P}}(t+\delta t) - u_{\mathrm{P}}(t)]. \tag{17}$$

(v) Calculate $\langle \epsilon_l^q \rangle$ by time averaging for the largest possible range of values of the exponent q, including for negative q.

(vi) Identify $\langle \epsilon_l^q \rangle$ with a *pure* power-law l^{τ_q} (times a constant) over the estimated inertial range. This is typically done by least-mean-squares fitting of $\log \langle \epsilon_l^q \rangle$ *vs.* $\log l$ to a linear function.

(vii) Perform a numerical Legendre transformation on τ_q to obtain $f(\alpha)$.

5. Shortcomings of the processing technique for $f(\alpha)$

In this Section, (i)–(vii) refer to the enumeration of the preceding Section.

Assumption (i) (finiteness of the viscosity) may produce a *spurious point* in the $f(\alpha)$ function:

$$\alpha = 1, \quad f(\alpha) = 1. \tag{18}$$

Indeed, let us assume that, in the one-dimensional cuts, there are quiescent regions in the flow, filling a finite fraction of space, where the velocity is regular in the following sense: there is no appreciable small-scale activity, so that the velocity gradients $\partial u/\partial x$, are $O(v_0/l_0)$. In the limit $\nu \to 0$ (assuming the limit exists) such regions do not contribute to the energy dissipation. Still, for finite ν, the local average $\epsilon_l(x)$ of the dissipation over a small distance l will be $O(\nu(v_0/l_0)^2)$, independent of l. By (13), this implies an exponent $\alpha = 1$ on a set of dimension $f(\alpha) = 1$. Equation (18) follows. We also observe that moments of negative order of the dissipation, which are infinite under the assumption of quiescent regions, will be rendered finite with spurious scaling as soon as some viscosity, however small, is present. Such phenomena are illustrated in §7 on Burgers' model.

The main shortcoming of (ii) is the assumption that the quantity $(\partial u/\partial x)^2$ is a faithful representative of the full dissipation, as far as scaling laws are concerned. Note that the scaling laws obtained with the squared vorticity and the squared deformation (involving respectively the antisymmetrical and the symmetrical parts of the tensor $\partial_i v_j$) need not be the same. For example, Brachet (1990) gives evidence (based on a high-resolution simulation of the Taylor–Green vortex) that the correlation function of the squared vorticity and that of the squared rate of strain have different scaling laws.

We have nothing to add to the well-known limitations of the Taylor hypothesis (iii).

The most serious shortcoming of (iv) has to do with the probe size. With current technology, hot-wire probes are usually of diameter of the order of 1 μm and length of the order of 1 mm. Thus, signals are smoothed over a distance of about 1 mm. The Kolmogorov microscale η_{K} for most flows for which measurements of $f(\alpha)$ have been attempted is between 0.1 and 1 mm (see, for example, table 1 of Meneveau & Sreenivasan 1991). This in itself is not necessarily a serious shortcoming, since the Kolmogorov microscale is about one order of magnitude smaller than the actual scale at which the energy spectrum begins to bend away from the $-\frac{5}{3}$ law (see, for example,

figure 75 of Monin & Yaglom 1975). The scale at which most of the mean dissipation resides, is typically a factor 20 larger than η_K. To obtain a well-resolved dissipation, experimentalists usually resort to probes no longer than $5\eta_K$.

A more serious difficulty in the present context is the following. Suppose one accepts the multifractal model, as is necessary to give a meaning to an $f(\alpha)$ measurement. Then, an unavoidable consequence is that the viscous cutoff, given by (11), is dependent on α. The smaller α, the smaller the viscous cutoff, particularly at high Reynolds numbers R. As an example, let us consider the wake and boundary-layer data analysed by Meneveau & Sreenivasan (1987, 1991). The corresponding Reynolds numbers, based on r.m.s. velocity fluctuations and integral scale, are respectively $R = 728$ and 967. They report, in figure 24 of their 1991 paper, values of α down to a minimum $\alpha_{\min} = 0.35$. We then have, by (11),

$$\frac{\eta_K}{\eta_{\min}} = R^{\frac{3}{3+\alpha_{\min}}-\frac{3}{4}} \approx R^{0.15}. \tag{19}$$

It follows that the minimum dissipation scale is 2.68 times (resp. 2.8 times) smaller than the Kolmogorov microscale for the wake (resp. the boundary layer). The actual numbers are $\eta_{\min} = 0.1$ mm (resp. $\eta_{\min} = 0.06$ mm) for the wake (resp. the boundary layer). The probe used in these experiments had a length of 0.7 mm. Thus the probe was 7 (resp. 12) times larger than the value of $\eta_{\min}$. It is not clear if such ratios are sufficiently small for the corresponding small-α events to be well resolved. It will be of interest to repeat the same experiments with probes shorter by at least a factor two or by non-intrusive high-resolution methods. Let us stress that the actual existence of dynamically significant events taking place on such minute scales depends heavily on the validity of the multifractal model (see §8).

Item (v) (time-averaging) is a well-known difficulty in experimental measurement of moments, especially for high-order ones. Similar problems, arising in the measurement of high-order structure functions are discussed in Anselmet *et al.* (1984).

Item (vi) (the identification of $\langle \epsilon_l^q \rangle$ with a pure power law) is a source of concern for large q. Equation (8) indicates that, for l sufficiently small compared to the integral scale and sufficiently large compared to dissipative scales, a pure power law is obtained to leading order. Yet, suppose that at finite Reynolds numbers there are correction terms involving a (suitable) dissipation scale η_q, so that, instead of (8), we have

$$\langle \epsilon_l^q \rangle \sim \left(\frac{v_0^3}{l_0}\right)^q \left(\frac{l}{l_0}\right)^{\tau_q} \left[1 + O\left(\frac{\eta_q}{l}\right)\right], \tag{20}$$

a correction which vanishes with η_q in the infinite Reynolds number limit. If the correction term has a positive sign, it will lead to underestimating the actual value of τ_q. An interesting example is provided by the Gaussian model discussed in §6, for which all the τ_q are zero because the asymptotics are dominated by the mean dissipation rate. Still, because of the admixture of l^{-1} terms (with a positive coefficient $O(q^2)$), the empirically determined τ_q may appear to have a non-trivial multifractal dependence on q, for large positive or negative q (see §6). The Gaussian model is directly relevant if the flow possesses quiescent regions in which the instrumental noise dominates over the very small viscous dissipation signal; moments of negative order of the dissipation are then rendered spuriously finite again, but by a mechanism different from that discussed above in connection with (i).

This could happen for example when the probe occasionally encounters irrotational fluid; however, such events were not detected in the experiments of Meneveau & Sreenivasan (Meneveau 1991, personal communication). The effect of weak noise on moments of positive order, on the other hand, appears to be negligibly small.

Item (vii) (the numerical inverse Legendre transform) can lead to various errors. The Legendre transform, when performed by a derivative technique, is ill-conditioned for noisy data. A more fundamental problem is the fact that the Legendre transform of a non-convex function is the same as the Legendre transform of its convex hull. Suppose, for example, that $f(\alpha)$ is defined only for discrete values α_i of α. An attempt to reconstruct $f(\alpha)$ from its Legendre transform τ_q will then produce, in addition to the discrete points $(\alpha_i, f(\alpha_i))$, the spurious line segments forming the convex hull of that set. An example of this effect, using Burgers' model, is discussed in §7. It is likely that the binning method mentioned at the end of §3 is more capable of revealing discrete points when they exist.

6. A Gaussian model

Our Gaussian model is intended to show how spurious multifractality can arise from *lack of asymptoticity*.

The Gaussian model is defined by a sequence of Gaussian random variables $s_j, j = 1, 2, \ldots$. The variables are assumed independent, real, of zero mean value and equal variance $\sigma^2 = \langle s_j^2 \rangle$. The variable s_j should be thought of as a time series sampled at $t = j\delta t$:

$$s(j\delta t) \equiv s_j. \tag{21}$$

Thus, the Gaussian model is just a discrete version of white noise.

In accordance with (17), we define the *local dissipation* as

$$\epsilon(j) \equiv (s_{j+1} - s_j)^2. \tag{22}$$

Note that constant factors, such as δt^{-2}, are irrelevant for the scaling properties. We also define the J-averaged dissipation, the discrete analogue of ϵ_l:

$$\epsilon_J \equiv \frac{1}{J} \sum_{j=1}^{J} \epsilon(j). \tag{23}$$

The scaling exponents τ_q for the Gaussian model are defined as usual in terms of the asymptotics of moments of the J-averaged dissipation:

$$\langle \epsilon_J^q \rangle \propto J^{\tau_q}, \quad J \to \infty. \tag{24}$$

The condition $J \to \infty$ selects 'inertial-range scales'. Indeed, in the Gaussian model, the dissipation scale is $O(1)$ and the integral scale is infinite. The interesting property of the Gaussian model is that the behaviour of moments of the J-averaged dissipation for large J has a simple expression (derived in the Appendix):

$$\langle \epsilon_J^q \rangle \approx (2\sigma^2)^q (1 + \tfrac{3}{2} q(q-1) J^{-1} + O(J^{-2})), \quad J \to \infty. \tag{25}$$

This expression is valid for both positive and negative integer q. The existence of moments of negative order when J is large enough is proved in the Appendix.

We observe that the leading-order behaviour of the qth moment of the J-averaged dissipation is simply the qth power of the average dissipation $2\sigma^2$. The correction term in (25) can also be obtained by evaluating the (approximately) Gaussian fluctuations of ϵ_J around its mean value.

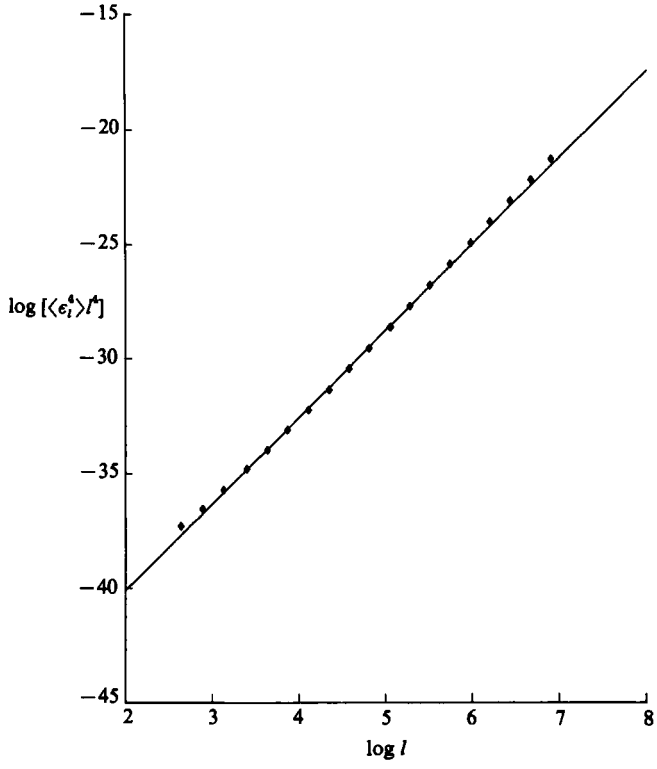

FIGURE 1. Fourth-order moment of the dissipation $\langle \epsilon_l^4 \rangle l^4$ obtained with the Gaussian model, in log–log coordinates. The straight line is a least-square fit to a power law over a range of scales of two decades. It gives a spurious exponent 3.8 instead of 4.

It follows from (24) and (25) that

$$\tau_q = 0, \quad \forall q. \tag{26}$$

Thus, from a scaling viewpoint the Gaussian model behaves as a uniform dissipation.

Suppose now that we try to measure the exponents τ_q from a numerical experiment in which we generate a large number of independent Gaussian random variables s_j. We can then try to obtain τ_q by plotting $\langle \epsilon_J^q \rangle$ *vs.* J in log–log coordinates and measuring the slope. It follows from (25) that pure scaling with the exponent $\tau_q = 0$ will be seen only if the correction term is negligible. The condition for this is seen to be

$$J \gg |q(q-1)|. \tag{27}$$

Thus, for large orders (positive or negative), it is necessary to have data over an increasing range of scales, growing proportionally to $|q|^2$. Otherwise, contamination by the subdominant terms will result in underestimating of the scaling exponents associated with large orders and hence to spurious intermittency.

To illustrate this phenomenon we shall now take Gaussian data and process them in a way similar to what is done with experimental turbulence data. In typical turbulence experiments involving hot-wire probes, the sampling frequency is between the frequency corresponding to the Kolmogorov dissipation scale η and one-tenth thereof. One way to delimitate the inertial range, suggested by Anselmet *et al.* (1984), is to plot the third-order structure function. One then identifies the range of

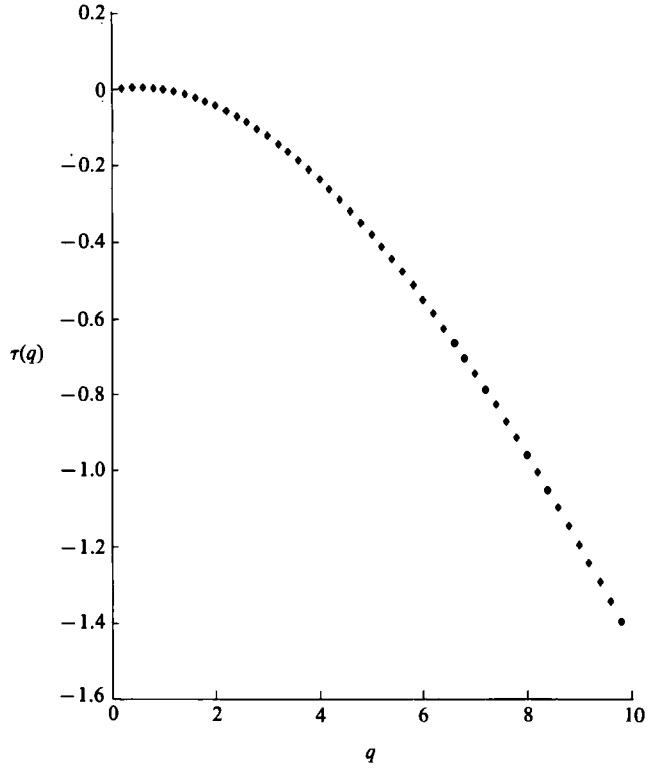

FIGURE 2. Variation of the (spurious) scaling exponent τ_q with the order of the moment. Same conditions as in figure 1. The graph of τ_q, being curved, implies spurious multifractality.

scales over which this structure function follows Kolmogorov's (1941*b*) $-\frac{4}{5}\epsilon l$ law. Typically, the bottom (smallest scale) of the inertial range is around 30η, corresponding to three to thirty successive samples. The position of the upper limit depends of course on the Reynolds number. For the highest Reynolds number data analysed in this way (Castaing, Gagne & Hopfinger 1990), the inertial range does not span more than two decades.

We were thus led to conceive the following computer experiment. We used our Gaussian model and measured the *apparent* scaling exponent of the moments of the dissipation over a range of values of J. This range begins at $J = 10$ (had we taken a smaller value, the spurious effects would be stronger; with a larger value they would be weaker) and extends over two decades. The (apparent) scaling exponents $\tau_q^{\rm app}$ for the moments of the dissipation of order up to ten are determined by least-square fits to a power law in logarithmic variables. An example is given in figure 1, where we have represented (in log–log coordinates) the fourth-order moment $\langle \epsilon_l^4 \rangle$, multiplied by l^4 to make the slope positive. The straight line, which is a least-square fit in the interval $10 \leqslant J \leqslant 1000$, has slope 3.8 ± 0.04. Hence $\tau_4^{\rm app} = -0.2 \pm 0.04$, instead of the correct value $\tau_4 = 0$. In figure 2, we represent the graph of $\tau_q^{\rm app}$ for $0 \leqslant q \leqslant 10$. It is seen to drop to increasingly negative values and displays curvature. The inverse Legendre transform (15) would then produce a spurious non-trivial $f(\alpha)$ spectrum.

7. Burgers' model

In this section we use Burgers' model to illustrate several possible shortcomings of the multifractal analysis. There is a considerable wealth of knowledge about this model. For what we need here, the main references are Burgers (1974), Hopf (1950), Cole (1951) and Fournier & Frisch (1983).

7.1. *Summary of key results for Burgers' model*

Burgers' equation can be written either in terms of a velocity field v as

$$\partial_t v(t,x)+v\,\partial_x v=\nu\,\partial_x^2 v, \tag{28}$$

or in terms of a stream function ψ such that

$$v=-\partial_x\psi. \tag{29}$$

The latter satisfies $$\partial_t\psi(t,x)-\tfrac{1}{2}(\partial_x\psi)^2=\nu\,\partial_x^2\psi. \tag{30}$$

The Hope–Cole transformation $$\psi=2\nu\ln\theta \tag{31}$$

reduces (30) to the heat equation

$$\partial_t\theta(t,x)=\nu\,\partial_x^2\theta. \tag{32}$$

In the absence of boundaries, the initial-value problem

$$\psi(0,x)=\psi_0(x) \tag{33}$$

has the following solution, a consequence of the Hopf–Cole transformation ($t>0$):

$$\psi(t,x)=2\nu\ln\left[\frac{1}{(4\pi\nu t)^{\frac{1}{2}}}\int_{-\infty}^{+\infty}\mathrm{d}y\exp\left(\frac{F(t,x,y)}{2\nu}\right)\right], \tag{34}$$

where $$F(t,x,y)=\psi_0(y)-\frac{(x-y)^2}{2t}. \tag{35}$$

From (34), it follows by a steepest-descent argument that in the inviscid limit

$$\psi(t,x)=\max_y F(t,x,y)\quad\text{for}\quad\nu\to 0. \tag{36}$$

In view of (35) this means that, in the inviscid limit, $\psi_0(y)-y^2/(2t)$ and $\psi(t,x)+x^2/(2t)$ are essentially Legendre transforms of each other.

When the initial condition has bounded velocity gradients, $\psi_0(y)-y^2/(2t)$ is convex in y, for sufficiently short times (because $-y^2/(2t)$ is large and convex and $\psi_0(y)$ has bounded second derivatives). For such times the Legendre transformation is smooth. After some time, singularities will develop, corresponding to those y where the convex hull of $\psi_0(y)-y^2/(2t)$ departs from the function itself. In terms of the velocity $v(t,x)$, this means that there are shocks, i.e. positions $x_i(t)$ where the velocity has a finite discontinuity.

Our interest will be in the typical behaviour of solutions for *random* initial conditions. Specifically, we assume that the initial conditions are random, homogeneous (statistical properties invariant under space-translations), have zero mean value and are smooth (for non-smooth initial conditions, see She, Frisch & Aurell 1992 and Sinai 1992) with a single lengthscale and a single velocity scale, both taken to be unity. An instance of this would be Gaussian initial conditions with zero mean value and a spectrum $\exp(-k^2)$. There is no need here to be too specific, since our arguments will be mostly phenomenological, a fully rigorous version of the

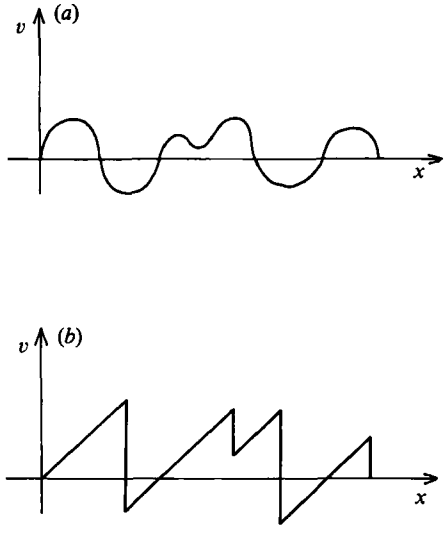

FIGURE 3. Sketch of the spatial structure of the solution to Burgers' equation in the inviscid limit with random initial conditions and all characteristic scales $O(1)$: (a) initial condition; (b) solution at $t = O(1)$.

subsequent arguments would of course need a hardening of the assumptions. We shall be interested in the solutions of Burgers' equation for times $O(1)$, sufficiently long to have formed shocks (for the very long-time regime, see Kida 1979). Figure 3 shows a typical sketch of the spatial aspect of the initial condition (in terms of the variable v) and of the evolved solution $v(t,x)$ after a time $O(1)$ in the inviscid limit.

The following properties of $v(t,x)$, for fixed $t = O(1)$, which are consequences of the Hopf–Cole solution, will be relevant for our subsequent arguments:

(i) $v(t,x)$ is a random homogeneous function of x with zero mean value;

(ii) $v(t,x)$ is smooth in x with $O(1)$ space derivatives, except at discrete points x_i;

(iii) the points x_i (shocks) are distributed homogeneously with $O(1)$ spacing between successive points;

(iv) at any point x_i the velocity has a negative discontinuity δv_i which is $O(1)$.

Note that the fact that everything is $O(1)$ is an immediate consequence of our choice of units. The above properties hold in the inviscid limit. If a finite small viscosity is assumed, (ii)–(iv) must be modified as follows:

(v) the above discontinuities are replaced by smooth, but steep transition regions with a tanh profile and a width $O(\nu)$, which for Burgers' model plays the role of the dissipation scale.

We mention that all the above properties are generally believed also to hold when Burgers' model includes a random force, such that all spatial, temporal and amplitude scales are $O(1)$.

Let us now consider the implications from the viewpoint of the multifractal analysis. We shall deal successively with the two multifractal approaches: structure functions (§7.2) and dissipation moments (§7.3). In each case, we consider first the inviscid limit and then the effect of a finite small viscosity. The notation used hereafter is consistent with our definitions for the Navier–Stokes case. For example, $\delta v_l(x)$ is the velocity increment (now a scalar) and $\epsilon_l(x)$ is the energy dissipation in an interval of length l centred around x, divided by l. All the statistical quantities will be evaluated for scales l in the inertial range, i.e. for

$$1 \gg l \gg \nu. \tag{37}$$

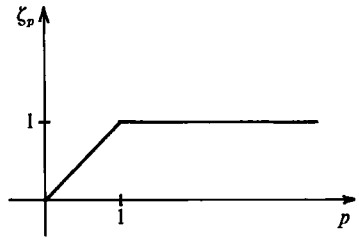

FIGURE 4. Exponents ζ_p of structure functions for Burgers' model.

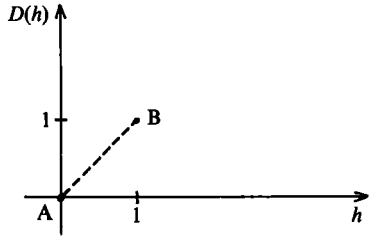

FIGURE 5. $D(h)$ function for Burgers' model. Points A and B are genuine. The segment is an artefact of the reconstruction by Legendre transformation.

7.2. *Structure functions for Burgers' model*

To evaluate the structure functions $\langle(\delta v_l)^p\rangle$, we must consider separately the contributions of shocks and of smooth regions. Since the inter-shock spacing is $O(1)$, in an interval of length l satisfying (37), there is a probability $O(l)$ of having a shock and $1-O(l) \approx 1$ of having no shock. In other words, the singularity structure of the velocity field is *bifractal*: there is a set of dimension $D = 0$ (the shocks) on which the singularity exponent is $h = 0$ (discontinuities) and another set of dimension $D = 1$ on which the exponent is $h = 1$ (regular behaviour). Hence, the structure functions of order $p > 0$ may be written (cf. §2)

$$\langle(\delta v_l)^p\rangle \sim c_1 l^1 + c_2 l^p, \tag{38}$$

where c_1 and c_2 are two $O(1)$ constants. For small l the power law with the smallest exponent dominates. Hence,

$$\langle(\delta v_l)^p\rangle \sim l^{\zeta_p}, \quad \zeta_p = \min(p, 1). \tag{39}$$

The graph of ζ_p given by (39) is shown in figure 4. If a finite small viscosity is included in the derivation, no modification is found to leading order (the situation will be different in §7.3).

We observe that (39) is just a special case of the Legendre transform formula (4), adapted to the one-dimensional case,

$$\zeta_p = \min_h (ph + 1 - D(h)). \tag{40}$$

Indeed, the function $D(h)$ has just two points A ($h = 0, D = 0$) and B ($h = 1, D = 1$).

An interesting observation can now be made. Suppose we wish to recover the function $D(h)$ by performing the inverse Legendre transform of (40):

$$1 - D(h) = \max_p (\zeta_p - ph). \tag{41}$$

A simple calculation then produces the function shown in the graph in figure 5. In addition to the two aforementioned points A and B, $D(h)$ has now a spurious segment of points joining them. This is because by performing a Legendre transform and then

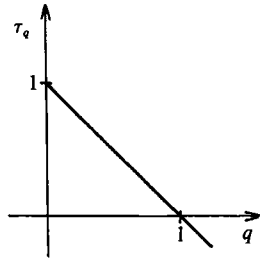

FIGURE 6. Exponents τ_q for moments of the space-averaged dissipation for Burgers' model (inviscid limit).

its inverse, we recover not the original function but its *convex hull*. Spurious results of this sort are known in other areas of dynamical systems (Grassberger *et al.* 1988; Artuso, Aurell & Cvitanović 1990*a*, *b*).

7.3. *Dissipation moments for Burgers' model*

We turn now to the moments of the space-averaged dissipation ϵ_l. It is here essential to distinguish the cases of vanishing viscosity and of small viscosity. In the former, all the dissipation is concentrated at the shocks ($\alpha = 0, f(\alpha) = 0$) while in the latter there is a residual small ($O(\nu)$) dissipation at regular points ($\alpha = 1, f(\alpha) = 1$).

We begin again with the inviscid limit. The probability of an interval of length $l \ll 1$ intercepting a shock is $O(l)$ (see §7.2). When a shock is present, the total dissipation in such an interval is $O(1)$ (it is proportional to the cube of the velocity discontinuity). It follows that moments of positive order q are given by

$$\langle (\epsilon_l)^q \rangle \sim l^{\tau_q}, \quad \tau_q = 1-q. \tag{42}$$

For negative q the moments are infinite, since there is a finite probability of having a vanishing dissipation in an interval of length l. The graph of τ_q given by (42) is shown in figure 6. Here, we detect an inconsistency with the relation (10) based on bridging the two multifractal formalisms via Kolmogorov's relation (9). Indeed, (10) and (42) imply

$$\zeta_p = 1, \tag{43}$$

which is identical to (39) only for $p \geqslant 1$. The reason for the discrepancy is that the $D(h)$ function has two points (see the beginning of §7.2) while the $f(\alpha)$ function has a single point, corresponding to shocks.

Turning now to the case of finite small viscosity, we obtain

$$\langle (\epsilon_l)^q \rangle \sim c_3 \nu^q l^0 + c_4 l^{1-q}, \tag{44}$$

where c_3 and c_4 are $O(1)$ constants. The first term on the right-hand side of (44) is the contribution of the residual $O(\nu)$ dissipation outside of the shocks, while the second comes from the shocks. If we were just to take the smallest exponent in (44) to find the small-l behaviour, we would obtain $\tau_q = 1-q$ for $q \geqslant 1$ and $\tau_q = 0$ for $q < 1$. This is however incorrect since we cannot take l smaller than the viscous cutoff, which is $O(\nu)$ (see (37)). Comparing the first and second terms on the right-hand side of (44), we find that the power law with exponent $1-q$ dominates for all $q > \frac{1}{2}$. For $q < \frac{1}{2}$, the first term in (44) dominates at sufficiently small inertial-range scales. We thus obtain

$$\tau_q = \begin{cases} 1-q & \text{for} \quad q > \frac{1}{2}; \\ 0 & \text{for} \quad q < \frac{1}{2}, \end{cases} \tag{45}$$

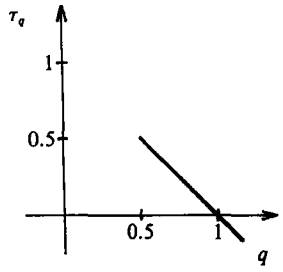

FIGURE 7. Same as figure 6 but including the effect of a finite small viscosity.

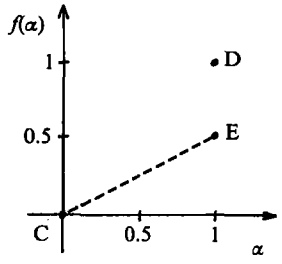

FIGURE 8. THE $f(\alpha)$ function for Burgers' model. Only point C is genuine. The point D and the segment C–E are artefacts of two reconstruction methods when a finite small viscosity is included.

the graph of which is shown in figure 7. Note that the moments of negative order have become finite through the effect of viscosity (in an interval of arbitrary small length l there is always a positive residual dissipation). Note also that the function τ_q is not convex.

If we try to reconstruct the function $f(\alpha)$ from τ_q, we have a choice between two evils. First, we can identify the different discrete slopes $s_1 = 0$ and $s_2 = 1$ present in the graph of τ_q. Each slope s_i corresponds to an exponent α such that $\alpha_i - 1 = s_i$; the associated dimension is given by $f(\alpha) = q(\alpha_i - 1) + 1 - \tau_q$. This method produces two points: C ($\alpha = 0, f(\alpha) = 0$) and D ($\alpha = 1, f(\alpha) = 1$) shown on figure 8. The point C associated to the shocks is genuine: it is also present in the inviscid limit. The point D is spurious and it is a finite-viscosity effect. Reducing the viscosity will not make it disappear. The second method for recovering $f(\alpha)$ is to perform the inverse Legendre transform given by (15). This produces the segment shown in figure 8, joining the point C to the point E ($\alpha = 1, f(\alpha) = \frac{1}{2}$). Except for the point C, the entire interval is now spurious.

8. Conclusion

We have found a variety of effects, not reported so far, which can affect the determination of the $f(\alpha)$ function from experimental turbulence data. If we assume that a multifractal description is appropriate for fully developed turbulence, we must also accept the consequences, such as the dependence of the viscous cutoff on the singularity exponent α and the implications for probe sizes discussed in §5. But we stress that there is still no conclusive evidence that the multifractal description (in either of the two 'standard' versions discussed in §2) is really adequate. One possible shortcoming of the standard versions comes from high-resolution numerical simulations which show that the smallest structures present in the flow are slender vortex filaments with circular cross-section (She, Jackson & Orszag 1990; Vincent & Meneguzzi 1991). (There is also some recent experimental evidence for these

filaments (Douady, Couder & Brachet 1991).) The nonlinear term in these filaments vanishes to leading order. It follows that their diameter is much larger than the scale obtained by balancing the local turnover time and the viscous diffusion time, as done in standard multifractal models.

By applying the existing multifractal processing techniques to the Gaussian model (§6) and to Burgers' model (§7), which are both exactly soluble, we have found possible sources of spurious $f(\alpha)$ due to finite Reynolds number effects, namely the contamination of leading-order scaling by subdominant terms and the spurious scaling induced by a residual finite viscosity in regions without any small-scale activity. Being aware of such effects, it may be possible to try to eliminate them, at least partially, by carefully comparing data with different Reynolds numbers. For subdominant corrections, one can assume that two power laws are simultaneously present. For viscous effects, one can try to identify spurious scaling in which the constants in front of the power laws display a dependence on viscosity.

We have also shown that obtaining the $f(\alpha)$ function for the dissipation and the $D(h)$ function characterizing multifractality of structure functions are in principle two distinct goals. We have shown on Burgers' model that the scaling properties of structure functions of order less than one cannot be inferred from the $f(\alpha)$ function. In figure 34 of Meneveau & Sreenivasan (1991) a comparison is made between directly measured exponents of structure functions from Anselmet *et al.* (1984) and those inferred via (9) from their measurements of the $f(\alpha)$ function. For low orders, both sets of data are very close to the Kolmogorov (1941*a*) prediction and thus in trivial agreement. For high orders, say beyond $p = 10$, the measurements of the ζ_p exponents are considered not fully reliable by Anselmet *et al.* (1984). The agreement can thus hardly be considered as conclusive evidence for multifractality. Moreover, direct experimental determination of structure functions and of $D(h)$ may involve difficulties beyond those already discussed in Anselmet *et al.* (1984).

We also mention that direct measurements of local scaling exponents by wavelet transform techniques have been attempted (Argoul *et al.* 1989; Bacry *et al.* 1990). Some of the difficulties associated with the interpretation of wavelet transforms were pointed out by Bacry *et al.* (1990). In addition, there are indications that this is a very noisy technique because it uses only local information, albeit over a wide range of scales (Vergassola *et al.* 1991).

Disentangling the (presumed) multifractal structure of fully developed turbulence is a very challenging task. The validation and the assessment of processing techniques for experimental data which has been the focus of the present paper is only one aspect. The development of state-of-the-art experiments, using smaller probes or non-intrusive high-resolution optical techniques (see e.g. Miles *et al.* 1989) associated with moderate to high Reynolds number flows may well completely upset our current views of fine-scale phenomena in fully developed turbulence.

We are grateful to C. Meneveau, M. Nelkin and V. Yakhot for discussions and suggestions. This work was supported by the EEC (SC1-0212-C) and by DRET (90/1444).

Appendix

In this Appendix we will discuss in more detail the solution of the Gaussian model defined in §6. For clarity, we recall that the model considers a sequence of Gaussian random variables s_j, $\{j = 1, 2, \ldots\}$, independent, real, with zero mean value

and having the same variance $\sigma^2 = \langle s_j^2 \rangle$. The local dissipation is defined as $\epsilon(j) \equiv (s_{j+1} - s_j)^2$ and the J-averaged dissipation as $\epsilon_J \equiv (1/J) \sum_{j=1}^{J} \epsilon(j)$. We are mainly interested in the asymptotic behaviour for $J \to \infty$ of the moments of the J-averaged dissipation. For convenience, we introduce the moments of the cumulated dissipation:

$$\Xi(J, q) = \langle (J\epsilon_J)^q \rangle. \tag{A 1}$$

A.1. *The generating function*

The most convenient way to obtain the asymptotic behaviour of the moments $\Xi(J, q)$ is through the generating function $\phi(z)$ of the random variable $J\epsilon_J$. By definition,

$$\phi(z) = \int \mathrm{d}s^J \left(\frac{1}{2\pi\sigma^2}\right)^{J/2} \exp\left(-\sum_{j=1}^{J} \frac{s_j^2}{2\sigma^2} - z \sum_{j=1}^{J} (s_{j+1} - s_j)^2\right), \tag{A 2}$$

where $\mathrm{d}s^J$ denotes integration over all of the J Gaussian variables. As usual, positive integer moments can be generated by taking derivatives of $\phi(z)$ at the point $z = 0$. In what follows, we shall impose periodic boundary conditions, whereby $s_{J+1} = s_1$. This is done for technical convenience and the corrections coming from this hypothesis affect neither the dominant nor the subdominant terms in the limit $J \to \infty$.

To evaluate the integral in (A 2), we introduce the new integration variables, $\hat{s}_m$, $\{j = 1, \ldots, J\}$ defined as the Fourier components of the discrete signal s_j, $\{j = 1, \ldots, J\}$:

$$s_j = \frac{1}{J^{\frac{1}{2}}} \sum_{m=1}^{J} \mathrm{e}^{\mathrm{i}k_m j} \hat{s}_m; \quad k_m = \frac{2\pi m}{J}. \tag{A 3}$$

Note that if J is odd then $\hat{s}_0$ is real, while the remaining $J-1$ variables consist of complex-conjugate pairs. If J is even, then $s_{J/2}$ is also real. Thus, the new integration variables are the independent real and imaginary components of the variables $\hat{s}_m$. Calling the (z-independent) Jacobian of this change of variables K, we then have

$$\begin{aligned}\phi(z) &= K \int \mathrm{d}\hat{s}_{\mathrm{r}}^{J/2}\, \mathrm{d}\hat{s}_{\mathrm{i}}^{J/2} \left(\frac{1}{2\pi\sigma^2}\right)^{J/2} \exp\left\{-\sum_{m=0}^{m=J/2} \left[\frac{1}{2\sigma^2} + 2z(1-\cos k_m)\right] [(\hat{s}_m^{\mathrm{r}})^2 + (s_m^{\mathrm{i}})^2]\right\} \\ &= K \prod_{m=0}^{J/2} \frac{1}{[1 + 4\sigma^2 z(1-\cos k_m)]}.\end{aligned} \tag{A 4}$$

Here, for convenience, we have taken J to be even. Real and imaginary are denoted by r and i respectively. The fact that $\phi(0) = 1$ (see (A 2)) implies that $K = 1$. Substituting the definition of k_m, taking advantage of the symmetry of the cosine and using the formula (1.3.94) of Gradshteyn & Ryzhik (1965) to express the resulting product in closed form, we obtain the final result

$$\phi(z) = \frac{2^J}{[(1 + 8\sigma^2 z)^{\frac{1}{2}} + 1]^J - [(1 + 8\sigma^2 z)^{\frac{1}{2}} - 1]^J}. \tag{A 5}$$

Here, we have again invoked the fact that $\phi(0) = 1$ to fix the correct signs. From (A 5), we immediately obtain the asymptotic form

$$\phi(z) \sim \left[\frac{2}{[(1 + 8\sigma^2 z)^{\frac{1}{2}} + 1]}\right]^J, \tag{A 6}$$

which is valid for $\mathrm{Re}\, z > 0$ and large J. Before considering explicit expressions for the moments, one simplifying observation can be made about the generating function.

Recall that the qth moment (for integer positive q) is determined by taking q-derivatives of the generating function with respect to z and then setting z to zero. A moment's inspection will show that exactly the same result is obtained using either (A 5) or the asymptotic form (A 6) provided that $q < J$.

A.2. *The positive moments*

We turn now to the determination of the asymptotic behaviour of the positive moments corresponding to $q > 0$. This can be done by analytically continuing the generating function, $\phi(z)$, into the complex plane and taking the inverse Fourier transform:

$$f(\epsilon) = \int_C \mathrm{d}z\, \mathrm{e}^{\mathrm{i}\epsilon z}\phi(\mathrm{i}z), \tag{A 7}$$

where the path, C, is defined by $z(C) = x + \mathrm{i}\delta$ with the real variable x ranging between $\pm\infty$ and with $\delta > 0$ being a fixed positive number. We are interested in the limit of large J, so that (A 6) can be used. It is now convenient to introduce a new integration variable

$$x = \left(\frac{\epsilon}{4\sigma^2}\right)^{\frac{1}{3}}[1 + (1 + \mathrm{i}8\sigma^2 z)^{\frac{1}{3}}]$$

in terms of which the function f becomes

$$f(\epsilon) = \frac{1}{\mathrm{i}\sigma^2}\left(\frac{\epsilon}{\sigma^2}\right)^{(J-1)/2}\int_{C'} \mathrm{d}x \exp\left[\frac{1}{2}x^2 - \left(\frac{\epsilon}{4\sigma^2}x\right)^{\frac{1}{3}}\right]\left[\left(\frac{4\sigma^2}{\epsilon}\right)^{\frac{1}{3}}x - 1\right]x^{-J}. \tag{A 8}$$

This integral can be recognized as a difference of parabolic cylinder functions (equation (19.5.4) of Abramowitz & Stegun 1965) which, by using a recursion formula (Abramowitz & Stegun, equation (19.6.4)), can finally be reduced to a closed form involving Whitaker's function (Abramowitz & Stegun, Section 19.3).

The function f can now be used to directly calculate the behaviour of the moments, provided that the condition $J > q$ mentioned at the end of the last section is satisfied. We will omit the details except to note that the necessary integral is given in equation (7.722.2) of Gradshteyn & Ryzhik (1965). The final result is

$$\Xi(J, q) = (2\sigma^2)^q J \frac{\Gamma(J + 2q)}{\Gamma(J + q + 1)}. \tag{A 9}$$

A.3. *The negative moments*

From (A 2), it is easy to show that the negative moments are related to the Mellin transform of the generating function as

$$\langle \epsilon^{-r} \rangle = \frac{1}{\Gamma(r)}\int_0^\infty \mathrm{d}z\, z^{r-1}\phi(z). \tag{A 10}$$

To evaluate this, we first write the exact expression for the generating function, (A 5), as

$$\phi(z) = 2^J[1 + (1 + 8\sigma^2 z)^{\frac{1}{3}}]^{-J}\sum_{a=0}^{\infty}\left[\frac{(1 + 8\sigma^2 z)^{\frac{1}{3}} - 1}{(1 + 8\sigma^2 z)^{\frac{1}{3}} + 1}\right]^{aJ}, \tag{A 11}$$

where this expansion is clearly convergent for $z > 0$. Substituting this expansion into (A 10), introducing the new integration variable $x = \frac{1}{2}[(1 + 8\sigma^2 z)^{\frac{1}{3}} + 1]$ and using the formula (3.191.2) of Gradshteyn & Ryzhik (1965) to evaluate the resulting integral, we find

$$\Xi(J, q) = (2\sigma^2)^q J \frac{\Gamma(J + 2q)}{\Gamma(q)}\sum_{a=0}^{\infty}\frac{\Gamma(aJ + q)}{\Gamma((a + 1)J + q + 1)}, \quad 0 > q > -J. \tag{A 12}$$

We see that, provided that the sample length J is sufficiently long, negative moments of arbitrary order exist.

The first term of the sum in (A 12) is exactly equal to (A 9), so that the expression for $\Xi(J, q)$, valid for both positive and negative q, is

$$\Xi(J, q) \sim (2\sigma^2)^q J \frac{\Gamma(J+2q)}{\Gamma(J+q+1)}. \tag{A 13}$$

Equation (25) of §6 immediately follows from (A 1) and (A 13).

REFERENCES

Abramowitz, M. & Stegun, I. A. 1965 *Handbook of Mathematical Functions*. Dover.

Anselmet, A., Gagne, Y., Hopfinger, E. J. & Antonia, R. A. 1984 High-order velocity structure functions in turbulent shear flows. *J. Fluid Mech.* **140**, 63.

Argoul, F., Arnéodo, A., Grasseau, G., Gagne, Y., Hopfinger, E. J. & Frisch, U. 1989 Wavelet analysis of turbulence reveals the multifractal nature of the Richardson cascade. *Nature* **338**, 51.

Artuso, R., Aurell, E. & Cvitanović, P. 1990*a* Recycling of strange sets: I. Cycle expansions. *Nonlinearity* **3**, 325.

Artuso, R., Aurell, E. & Cvitanović, P. 1990*b* Recycling of strange sets: II. Applications. *Nonlinearity* **3**, 361.

Bacry, E., Arnéodo, A., Frisch, U., Gagne, Y. & Hopfinger, E. J. 1990 Wavelet analysis of fully developed turbulence data and measurement of scaling exponents. In *Turbulence and Coherent Structures* (ed. O. Métais & M. Lesieur), pp. 203–215. Kluwer.

Bensimon, D., Jensen, M. H. & Kadanoff, L. P. 1986 Renormalization-group analysis of the global structure of the period-doubling attractor. *Phys. Rev.* A **33**, 3622.

Benzi, R., Paladin, G., Parisi, G. & Vulpiani, A. 1984 On the multifractal nature of fully developed turbulence and chaotic systems. *J. Phys. Paris* A **17**, 3521.

Brachet, M. E. 1990 Géométrie des structures à petite échelle dans le vortex de Taylor–Green. *C. R. Acad. Sci. Paris* **311**, 775.

Burgers, J. M. 1974 *The Nonlinear Diffusion Equation*. D. Reidel.

Castaing, B., Gagne, Y. & Hopfinger, E. J. 1990 Velocity probability density functions of high Reynolds number turbulence. *Physica* D **46**, 177.

Cole, J. D. 1951 On a quasi-linear parabolic equation occurring in aerodynamics. *Q. Appl. Maths* **9**, 225.

Douady, S., Couder, Y. & Brachet, M. E. 1991 Direct observation of the intermittency of intense vorticity filaments in turbulence. *Phys. Rev. Lett.* **67**, 983.

Fournier, J. D. & Frisch, U. 1983 L'équation de Burgers déterministe et statistique. *J. Méc. Théor. Appl.* **2**, 699.

Frisch, U. 1991 From global scaling, *à la* Kolmogorov, to local multifractal scaling in developed turbulence. *Proc. R. Soc. Lond.* A **434**, 89.

Frisch, U. & Vergassola, M. 1991 A prediction of the multifractal model: the intermediate dissipation range. *Europhys. Lett.* **14**, 439.

Gagne, Y. & Castaing, B. 1991 Une représentation universelle sans invariance globale d'échelle des spectres d'énergie en turbulence développée. *C. R. Acad. Sci. Paris* **312**, 414.

Glazier, J. A., Jensen, M. H., Libchaber, A. & Stavans, J. 1986 Structure of Arnold tongues and the $f(\alpha)$ spectrum for period-doubling: experimental results. *Phys. Rev.* A **34**, 1621.

Gradshteyn, I. S. & Ryzhik, I. M. 1965 *Table of Integrals, Series and Products*. Academic.

Grassberger, P., Badii, R. & Politi, A. 1988 Scaling laws for invariant measures on hyperbolic and nonhyperbolic attractors. *J. Stat. Phys.* **51**, 135.

Halsey, T. C., Jensen, M. H., Kadanoff, L. P., Procaccia, I. & Shraiman, B. I. 1986 Fractal measures and their singularities: the characterization of strange sets. *Phys. Rev.* A **33**, 1141.

Hopf, E. 1950 The partial differential equation $u_t + uu_x = u_{xx}$. *Commun. Pure Appl. Maths* **3**, 201.

KIDA, S. 1979 Asymptotic properties of Burgers turbulence. *J. Fluid Mech.* **93**, 337.

KOLMOGOROV, A. N. 1941*a* The local structure of turbulence in incompressible viscous fluid for very large Reynolds numbers. *Dokl. Akad. Nauk SSSR* **30**, 301.

KOLMOGOROV, A. N. 1941*b* Dissipation of energy under locally isotropic turbulence. *Dokl. Akad. Nauk SSSR* **32**, 16.

KOLMOGOROV, A. N. 1962 A refinement of previously hypotheses concerning the local structure of turbulence in a viscous incompressible fluid at high Reynolds number. *J. Fluid Mech.* **13**, 82.

MANDELBROT, B. 1974 Intermittent turbulence in self-similar cascades: divergence of high moments and dimension of the carrier. *J. Fluid Mech.* **62**, 331.

MANDELBROT, B. 1991 Random multifractals: negative dimensions and the resulting limitations of the thermodynamic formalism. *Proc. R. Soc. Lond.* A **434**, 79.

MENEVEAU, C. M. & NELKIN, M. 1989 Attractor size in intermittent turbulence. *Phys. Rev.* A **39**, 3732.

MENEVEAU, C. M. & SREENIVASAN, K. R. 1987 The multifractal spectrum of the dissipation field in turbulent flows. *Nucl. Phys.* B *Proc. Suppl.* **2**, 49.

MENEVEAU, C. M. & SREENIVASAN, K. R. 1989 Measurement of $f(\alpha)$ from scaling of hystograms and applications to dynamical systems and turbulence. *Phys. Lett.* A **137**, 103–112.

MENEVEAU, C. M. & SREENIVASAN, K. R. 1991 The multifractal nature of turbulent energy dissipation. *J. Fluid Mech.* **224**, 429.

MILES, R. B., CONNORS, J. J., MARKOVITZ, E. C., HOWARD, P. J. & ROTH, G. J. 1989 Instantaneous profiles and turbulence statistics of supersonic free shear layers by Raman excitation plus laser-induced electronic fluorescence (Relief) velocity tagging of oxygen. *Expts Fluids* **8**, 17.

MILLER, P. & DIMOTAKIS, P. 1991 Stochastic geometric properties of scalar interfaces in turbulent jets. *Phys. Fluids* A **3**, 168.

MONIN, A. S. & YAGLOM, A. M. 1975 *Statistical Fluid Mechanics*, vol. 2 (Ed. J. Lumley). MIT Press.

OBOUKHOV, A. M. 1962 Some specific features of atmospheric turbulence. *J. Fluid Mech.* **13**, 77.

PALADIN, G. & VULPIANI, A. 1987 Degrees of freedom of turbulence. *Phys. Rev.* A **35**, 1971.

PARISI, G. & FRISCH, U. 1985 On the singularity spectrum of fully developed turbulence. In *Turbulence and Predictability in Geophysical Fluid Dynamics, Proc. Intl School of Physics 'E. Fermi', 1983, Varenna, Italy* (ed. M. Ghil, R. Benzi & G. Parisi), p. 84. North-Holland.

POLITI, A., BADII, R. & GRASSBERGER, P. 1988 On the geometric structure of non-hyperbolic attractors. *J. Phys.* A: *Math. Gen.* **21**, 763.

PRASAD, R. R., MENEVEAU, C. & SREENIVASAN, K. R. 1989 The multifractal nature of the dissipation field of passive scalars in fully turbulent flows. *Phys. Rev. Lett.* **61**, 74.

SHE, Z. S., FRISCH, U. & AURELL, E. 1992 The inviscid Burgers equation with initial data of Brownian type. *Commun. Math. Phys.* (submitted).

SHE, Z. S., JACKSON, E. & ORSZAG, S. A. 1990 Intermittent vortex structures in homogeneous isotropic turbulence. *Nature* **344**, 226.

SINAI, Y. 1992 Statistics of shock waves in solutions of the inviscid Burgers equation. *Commun. Math. Phys.* (submitted).

VERGASSOLA, M., BENZI, R., BIFERALE, L. & PISARENKO, D. 1991 Wavelet analysis of a Gaussian Kolmogorov signal. *Wavelets and Turbulence, Proc. USA–French Workshop, 1991, Princeton University, USA* (submitted).

VINCENT, A. & MENEGUZZI, M. 1991 The spatial structure and statistical properties of homogeneous turbulence. *J. Fluid Mech.* **225**, 1.

VAN DE WATER, W., VAN DER VORST, B. & VAN DE WETERING, E. 1991 Multiscaling of turbulent structure functions. *Europhys. Lett.* **16**, 443.

WU, X. Z., KADANOFF, L., LIBCHABER, A. & SANO, M. 1990 Frequency power spectrum of temperature fluctuations in free convection. *Phys. Rev. Lett.* **64**, 2140.